Adaptive quaternion control of a 3-DOF inertial stabilised platforms

Aurélien Cabarbaye, Rogelio Lozano, Moisés Bonilla Estrada

Adaptive quaternion control of a 3-DOF inertial stabilised platforms

Aurélien Cabarbaye[a,b], Rogelio Lozano[a,c] and Moisés Bonilla Estrada[d]

[a]UMI LAFMIA laboratory, CINVESTAV, 07360 Ciudad de México, D.F., México; [b]ISAE SUPAERO, 31400 Toulouse, France; [c]CNRS UMR, Sorbonne Universités, Universités de Technologie de Compiegne, 7253 Heudiasyc, France; [d]Department of automatic control, UMI 3175 CINVESTAV-CNRS, 07360 Ciudad de México, D.F., México

ABSTRACT

Inertial stabilised platforms are increasingly popular with a large range of products available mainstream. Most items are controlled using popular algorithms that sometimes do not offer best achievable performances. Present paper proposes an advanced control which aims at improving these latter. The exposed solution is based on quaternion representation and self-adapts to the characteristics of the payload it tries to stabilise. Proposed control law ensures the stability of the system whatever the required orientation path is. Although only simulation has been performed to check the performances of such control, results look very promising compared to non-adaptive controls and may help to construct more polyvalent and efficient gimbals which would further facilitate their expansion. Proposed control law can also be applied, as is, to every system that shares the same quaternion-based rotational dynamics.

1. Introduction

Inertial stabilised platforms (ISP) are mechanical structures designed to control the inertial orientation of their payload (Hilkert, 2008).

Such systems are used for a large range of applications. If they are currently well known for video applications as SportCam stabilised sticks or airborne camera mounts, they are likely to be adopted whenever a precise orientation of the payload is required (e.g. antennas, laser).

There are many kinds of ISP controls. If high-end systems take the payload deformation into account to ensure the highest possible accuracy (Hilkert, 2008), present article focuses on more affordable systems and intends to improve their effectiveness.

Some stabilisation systems take advantage of a movable optical element (e.g. actuated mirror, fluid lens) to stabilise the image of an optical payload, which provides a very fast reactivity but a limited orientation range. However, most systems are designed to move their entire payload so that it points its line of sight (LOS) to a particular target. Such mechanism is usually based on a gimbal architecture. If it does not offer a reactivity as good as previously mentioned solutions due to the heavier weight in motion, it offers a greater orientation range. Present paper deals with latter approach.

The easiest way to design an ISP control is to consider the three-motor axes independently. Azimuth and elevation are each controlled by a motor in a 2-DOF system (Khodadadi, Motlagh, & Gorji, 2011). These two motors are supplemented by an additional one, dedicated to payload yaw angle stabilisation, in a 3-DOF system. These controls are usually based on Euler angle representation (Hilkert, 2008). Although this representation is the most intuitive as it associates each rotation axis to a motor, it presents some drawbacks (e.g. instability around the gimbal lock), shared with Rodrigues and modified Rodrigues parameters representations (Chaturvedi, Sanyal, & McClamroch, 2011).

Those defects can be corrected using quaternion-based representation (Morais, Georgiev, & Sprößig, 2014). Nevertheless, the control input definition is less intuitive using this representation, particularly when ensuring payload roll is correctly orientated (i.e. for 3-DOF systems), and its non-unicity brings about instability issues (cf. homoclinic-like orbit) (Chaturvedi et al., 2011).

Rotation matrix representation does not present those drawbacks and is, by the way, used for numerous attitude controls (Lee, Leoky, & McClamroch, 2010; Raptis, Valavanis, & Moreno, 2011). However, it seems to require more computing power than using quaternions. This may explain why those latter are often used to parametrise it (Mayhew, Sanfelice, & Teel, 2009).

Whatever the adopted representation, the platform stabilisation dynamics is greatly related to the inertia matrix of the payload which affects the control responsiveness. Several adaptive controls have hence been proposed based either on Euler angles (Hilkert & Hullender, 1990; Li & Hullender, 1998) or rotation matrix (Lee, 2013) representations. The use of both representations implies previously detailed limitations.

The authors have otherwise proposed a fast computing ISP control based on axis-angle representation (Cabarbaye, Leal, Fabiani, & Estrada, 2017) that self-adapts to the payload it accommodates. A modified control is proposed in this article to improve its performances. It is still based on axis-angle

representation for low computing power reasons. However, the Math representation is modified in Section 2 to protect the algorithm from homoclinic-like orbit issue (Chaturvedi et al., 2011) and provides the quaternion expression of the required trajectory for extending the stability proof. The control scheme is presented in Section 3 where the adaptive law is made robust to the payload rotation speed. A simulation of the proposed control is exposed in Section 4. Projections of the obtained general control torque onto each motor axis is lastly provided in Section 5.

2. ISP mathematical representation

2.1 Specifications

Correct orientation of the payload is the main issue of an ISP control. The gimbal control must fulfil the two following requirements:

- Point the LOS of the payload to the desired direction
- Keep the roll angle of the payload to zero.

Both requirements are exposed in Figure 1.

In terms of vectors, it can be expressed, as follows:

- *LOS* must be collinear with the desired direction vector which goes from the payload lens to the target.
- Gravity vector (i.e. vector collinear to the earth gravity force) must be part of the plane passing through *LOS* and payload vertical vector.

This can be carried out via two successive rotations detailed hereafter.

Figure 1. Gimbal attitude parameters.

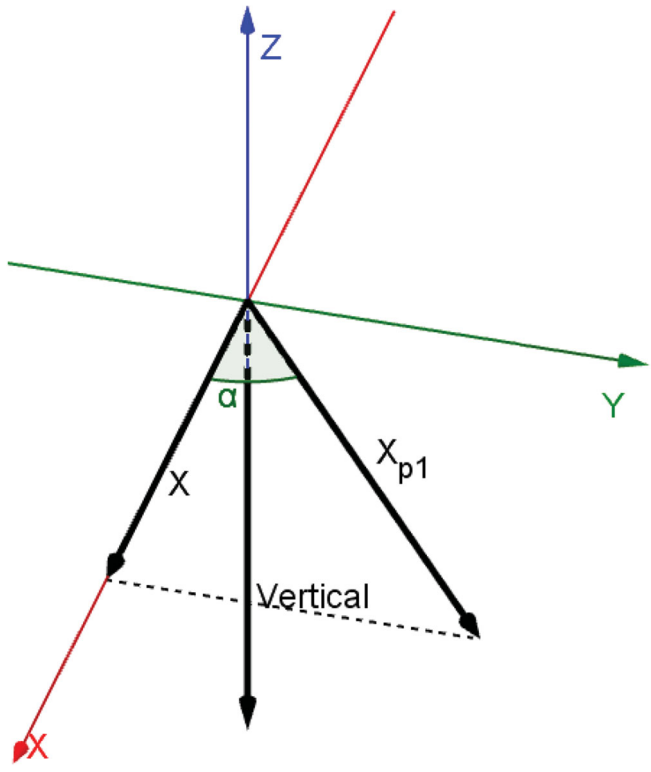

Figure 2. First rotation.

The supporting vector of the *LOS* being of the form: $X_{p2} = \begin{bmatrix} lx_{LOS} \\ y_{LOS} \\ z_{LOS} \end{bmatrix}$, the following vectors are defined:

$$X = \begin{bmatrix} x_{LOS} \\ 0 \\ 0 \end{bmatrix}, X_{p1} = \begin{bmatrix} x_{LOS} \\ y_{LOS} \\ 0 \end{bmatrix}.$$

The first rotation is performed to convert X-axis (i.e. X vector) into the transitional axis (i.e. X_{p1} vector). The quaternion representing the rotation between those two vectors is defined, as follows (Carino, Abaunza, & Castillo, 2015):

$$q_1' = \begin{bmatrix} X \cdot X_{p1} + \|X\| \left\|X_{p1}\right\| \\ X \times X_{p1} \end{bmatrix}$$

$$q_1 = \frac{q_1'}{\|q_1'\|}.$$

This rotation is the shortest that transforms a vector to another. It thus takes place around Z-axis. Therefore, the vertical vector is not modified. The result of such rotation is shown in Figure 2.

The second rotation follows the same idea as the first one. It is defined to transform the transitional vector (i.e. X_{p1} vector) onto *LOS* (i.e. X_{p2} vector), The rotation is defined as (Carino et al., 2015)

$$q_2' = \begin{bmatrix} X_{p1} \cdot X_{p2} + \left\|X_{p1}\right\| \left\|X_{p2}\right\| \\ X_{p1} \times X_{p2} \end{bmatrix}$$

$$q_2 = \frac{q_2'}{\|q_2'\|}.$$

The second rotation is shown in Figure 3.

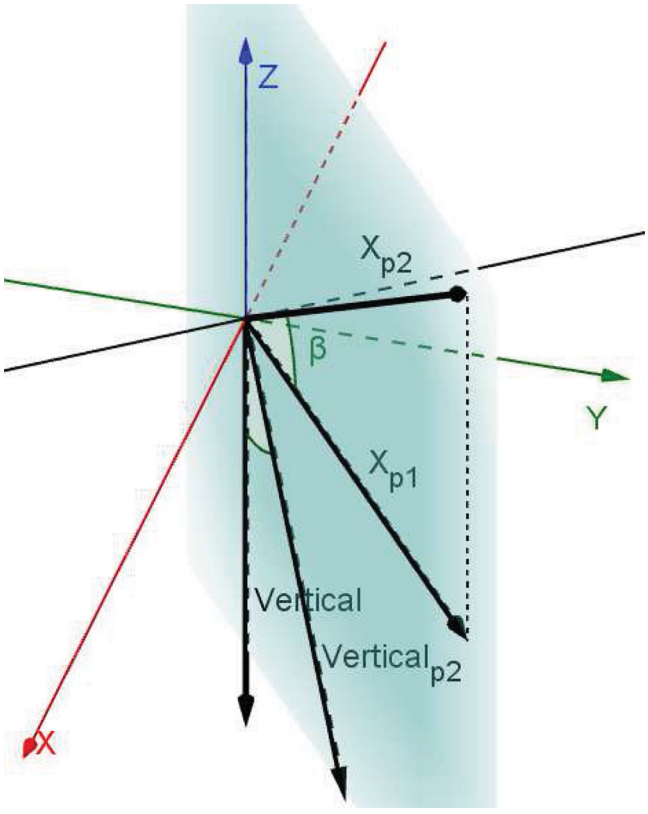

Figure 3. Second rotation.

Notice that the projection of the vertical vector (i.e. $Vertical_{p2}$ vector) is well within the plane formed by vertical vector and *LOS*. The result of both rotations is shown in Figure 4.

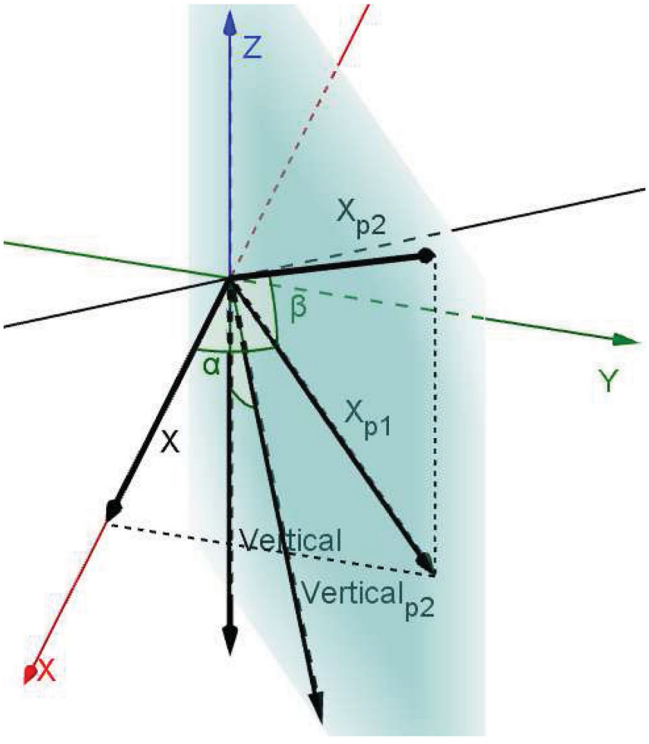

Figure 4. All rotations.

Observe that all requirements are fulfilled. The entire rotation is thus expressed by the quaternion obtained by the Hamilton product, noted $\otimes$ (Morais et al., 2014), of the two

$$q_d = q_2 \otimes q_1. \tag{1}$$

2.2 Dynamics

According to Goldstein (1962), quaternion-based rotational dynamics of the payload, assumed as rigid body, is

$$\begin{bmatrix} \dot{q} \\ \dot{\omega} \end{bmatrix} = \begin{bmatrix} \frac{1}{2} q \otimes \omega \\ J^{-1} (\tau - \omega \times J\omega) \end{bmatrix},$$

which combined with Equation (2),

$$\theta = 2 \ln q \tag{2}$$

gives

$$\begin{bmatrix} \dot{\theta} \\ \dot{\omega} \end{bmatrix} = \begin{bmatrix} \omega \\ J^{-1}\tau - J^{-1}\omega \times J\omega \end{bmatrix}. \tag{3}$$

3. Control

A simple PID could satisfactorily control the ISP making Equation (3) linear, defining

$$U = \tau - \omega \times J\omega. \tag{4}$$

However, most gimbal systems are designed to accommodate various sizes of payload (a wide range of camera models for instance) that present as many different inertial matrices J. Without an unpractical tweaking of control gains, those matrices must be fixed high enough, following a robust control approach, to ensure the stability of the whole system and so, even for the highest expected payload inertia matrix. A small payload would thus imply an unnecessary high control responsiveness which would come out as high power consumption. An adaptive control is hence designed in this section to assess J matrix and offer fine homogeneous moves. According to equation (3), the system is under actuated. The control of θ is therefore designed in Section 3.1, assuming that the state variable ω is its control input. In Section 3.2, the control of ω is built following an adaptive approach for the unknown J inertia matrix.

The payload inertia matrix J can be defined as

$$J = \begin{bmatrix} I_{xx} & I_{xy} & I_{xz} \\ I_{xy} & I_{yy} & I_{yz} \\ I_{xz} & I_{yz} & I_{zz} \end{bmatrix}.$$

ISP system being designed for a camera, some assessment can be made about J:

Hypothesis 3.1:

- $I_{ii} > 0 \, \forall i \in [1, 3]$
- $I_{ii} >> I_{ij} \, \forall (i, j) \in [1, 3]$.

3.1 θ control law design

3.1.1 θ stability condition

Equation (3) gives

$$\dot{\theta} = \omega. \tag{5}$$

Control error e_θ is defined for θ

$$e_\theta = \theta - \theta_d, \tag{6}$$

where θ_d is the expected orientation. In order to further reduce the required computational power, Equations (2) and (6) are combined

$$e_\theta = 2\ln q - 2\ln q_d = 2\ln(q \otimes q_d^*), \tag{7}$$

where q_d is given by Equation (1) and q is given by the attitude sensor of the payload[1]. Remark that this error is actually non-continuous around zero since $|e_\theta|$ is defined in the interval $[0, 2\pi]$. This may bring about instabilities to the ISP systems (cf. similar to the homoclinic-like orbit exposed by Chaturvedi et al. (2011)). This is solved slightly modifying function *ln*

$$2\ln(q) = \begin{cases} \begin{cases} \text{sgn}(\mathbf{q})(2 \cdot \arccos(q_0)), \ \textit{if } q_0 > 0 \\ \text{sgn}(\mathbf{q})(2 \cdot \arccos(q_0) - 2 \cdot \pi), \quad \textit{if } q_0 \leq 0 \end{cases} & , \textit{ if } |\mathbf{q}| \neq 0 \\ \mathbf{0}, \textit{ if } |\mathbf{q}| = 0 \end{cases}$$

noting $q = \begin{bmatrix} q_0 \\ \mathbf{q} \end{bmatrix}$.

The discontinuity takes place here at $|e_\theta| = \pi$ which becomes an unstable node thanks to the control law. Check that $2\ln(q) = 2\ln(-q)$, it ensures the stability condition (Chaturvedi et al., 2011): $u(q, \omega) = u(-q, \omega)$.

Combining Equations (5) and (6), it leads to

$$\dot{e}_\theta = \omega - \dot{\theta}_d. \tag{8}$$

Lemma 3.2: *The provisional control $\omega = -K_\theta e_\theta + \dot{\theta}_d$ can stabilise e_θ (K_θ is defined strictly positive).*

The expected control ω_d is therefore defined as

$$\omega_d = -K_\theta e_\theta + \dot{\theta}_d. \tag{9}$$

In order to keep the algorithm light, $\dot{\theta}_d$ is estimated thanks to the quaternion derivation (Morais et al., 2014)

$$\dot{q}_d = \frac{1}{2} q \otimes \dot{\theta}_d,$$

which gives

$$\dot{\theta}_d = 2q^* \otimes \dot{q}_d.$$

3.1.2 Condition on ω

Here ω control is studied in order to cancel error $e_\omega = \omega - \omega_d$. Equation (8) becomes

$$\dot{e}_\theta = \omega_d + e_\omega - \dot{\theta}_d$$

Introducing Equation (9) into the above gives

$$\dot{e}_\theta = -K_\theta e_\theta + e_\omega. \tag{10}$$

Equation (3) leads to

$$\dot{\omega} = J^{-1}\tau - J^{-1}\omega \times J\omega.$$

In term of error dynamics, it gives

$$\dot{e}_\omega = J^{-1}\tau - J^{-1}\omega \times J\omega - \dot{\omega}_d. \tag{11}$$

Define matrices J_1 and J_2

$$J_1 = \begin{bmatrix} I_{xx} & 0 & 0 \\ 0 & I_{yy} & 0 \\ 0 & 0 & I_{zz} \end{bmatrix}, \ J_2 = \begin{bmatrix} 0 & I_{xy} & I_{xz} \\ I_{xy} & 0 & I_{yz} \\ I_{xz} & I_{yz} & 0 \end{bmatrix}$$

such that $J = J_1 + J_2$. $\omega \times J\omega$ satisfies matching condition (Khalil, 1996). It verifies

$$\|\omega \times J\omega\| \leq \|J_1\omega\| \, \|\omega\| + \|J_2\omega\| \, \|\omega\| .$$

From assumption 3.1, it leads to

$$\|\omega \times J\omega\| \leq \text{sgn}\,(\omega)^{\mathrm{T}} J_1 \omega \, \|\omega\| + \|J_2\|_{\max} \, \|\omega\|^2 , \tag{12}$$

where $\|J_2\|_{\max}$ is the highest matrix norm in the range of payload that the ISP system is designed for.

3.2 ω adaptive control law design

Two general approaches of adaptive control are (Slotine & Li, 1991):

- Model-Reference Adaptive Control (MRAC)
- Self-Tuning Controllers (STC).

On the first hand, STC controls often require to introduce perturbation signals in the input to ensure their stability and convergence, which would be detrimental for the intended applications. On the second hand, MRAC controls do not necessarily supply the real parameter values. They indeed only provide acceptable values that ensure the stability of the system. However, since there is no need for proper parameters estimation, MRAC control approach is chosen.

3.2.1 Control law definition

The aim of the control is to reduce the magnitude of e_ω. In order to do so, the following relation is proposed and must be satisfied by the error control:

$$\dot{e}_\omega = -K_\omega e_\omega, \tag{13}$$

where K_ω is the control gain defined positive.

Combining Equations (13) and (11), it leads to

$$\tau = J\left(\dot{\omega}_d - K_\omega e_\omega\right) + \omega \times J\omega. \tag{14}$$

Lemma 3.3: *A control complying with Equation* (15) *stabilises system (3)*

$$\tau = \hat{J}\left(\dot{\omega}_d - K_\omega e_\omega\right) - e_\theta - \operatorname{sgn}\left(\mathrm{e}_\omega\right)\left(\operatorname{sgn}\left(\omega\right)^{\mathrm{T}} \hat{J}_1 \omega \left\|\omega\right\| + \left\|J_2\right\|_{\max} \left\|\omega\right\|^2\right), \tag{15}$$

where $\hat{J}$ is the estimated inertial matrix. $\hat{J}_1$ and $\hat{J}_2$ are defined such that $\hat{J} = \hat{J}_1 + \hat{J}_2$.

Notice that the control consists of two parts:

- A proportional part that intends to decrease the position error
- A part that can be assimilated as a Sliding Mode which aims at compensating the error increasing with ω.

The second part of the control could have been designed without splitting the inertia matrix in two. That is to say, following the expression:

$$-\operatorname{sgn}\left(\mathrm{e}_\omega\right) \left\|J\right\|_{\max} \left\|\omega\right\|^2.$$

However, according to assumption 3.1, $\left\|J_2\right\|_{\max} << \left\|J_1\right\|_{\max}$, the Sliding Mode part would have been of much greater importance and resulting trajectory would not have been smooth enough.

3.2.2 Control error estimation

Including the estimation errors of the inertial matrix: $\tilde{J} = \hat{J} - J$, Equation (15) of assumption 3.3 becomes

$$\begin{aligned}\tau = {} & \tilde{J}\left(\dot{\omega}_d - K_\omega e_\omega\right) + J\left(\dot{\omega}_d - K_\omega e_\omega\right) - e_\theta \\ & - \operatorname{sgn}\left(\mathrm{e}_\omega\right)\left(\operatorname{sgn}\left(\omega\right)^{\mathrm{T}} \tilde{J}_1 \omega \left\|\omega\right\| + \operatorname{sgn}\left(\omega\right)^{\mathrm{T}} J_1 \omega \left\|\omega\right\| \right. \\ & \left. + \left\|J_2\right\|_{\max} \left\|\omega\right\|^2\right).\end{aligned} \tag{16}$$

Substituting Equation (16) into equation (11), it gives

$$\begin{aligned}\dot{e}_\omega = {} & J^{-1}\tilde{J}\left(\dot{\omega}_d - K_\omega e_\omega\right) + J^{-1}J\left(\dot{\omega}_d - K_\omega e_\omega\right) - J^{-1}e_\theta \\ & - J^{-1}\operatorname{sgn}\left(\mathrm{e}_\omega\right)\left(\operatorname{sgn}\left(\omega\right)^{\mathrm{T}} \tilde{J}_1 \omega \left\|\omega\right\| + \operatorname{sgn}\left(\omega\right)^{\mathrm{T}} J_1 \omega \left\|\omega\right\| \right. \\ & \left. + \left\|J_2\right\|_{\max} \left\|\omega\right\|^2\right) \\ & - J^{-1}\omega \times J\omega - \dot{\omega}_d \\ = {} & -K_\omega e_\omega + J^{-1}\tilde{J}\left(\dot{\omega}_d - K_\omega e_\omega\right) - J^{-1}e_\theta \\ & - J^{-1}\operatorname{sgn}\left(\mathrm{e}_\omega\right)\left(\operatorname{sgn}\left(\omega\right)^{\mathrm{T}} \tilde{J}_1 \omega \left\|\omega\right\| + \operatorname{sgn}\left(\omega\right)^{\mathrm{T}} J_1 \omega \left\|\omega\right\| \right. \\ & \left. + \left\|J_2\right\|_{\max} \left\|\omega\right\|^2\right) \\ & - J^{-1}\omega \times J\omega.\end{aligned} \tag{17}$$

3.3 Adaptive law based on Lyapunov function

Theorem 3.4: *A sufficient stability condition consists in computing $\hat{J}$ by summing Equations* (18) *and* (19) *results.*

$$\dot{\hat{J}}_1 = \left\|\omega\right\| \operatorname{sgn}\left(\omega\right) \operatorname{sgn}\left(\mathrm{e}_\omega\right)^{\mathrm{T}} e_\omega \omega^{\mathrm{T}} \Gamma_1^{\mathrm{T}} - e_\omega \left(\dot{\omega}_d - K_\omega e_\omega\right)^{\mathrm{T}} \Gamma_1^{\mathrm{T}} \tag{18}$$

$$\dot{\hat{J}}_2 = -e_\omega \left(\dot{\omega}_d - K_\omega e_\omega\right)^{\mathrm{T}} \Gamma_2^{\mathrm{T}}. \tag{19}$$

Proof: The following Lyapunov function candidate is proposed

$$V = \frac{1}{2}\mathrm{e}_\theta^{\mathrm{T}} e_\theta + \frac{1}{2}\mathrm{e}_\omega^{\mathrm{T}} J e_\omega + tr\left(\tilde{J}_1 \Gamma_1^{-1} \tilde{J}_1^{\mathrm{T}} + \tilde{J}_2 \Gamma_2^{-1} \tilde{J}_2^{\mathrm{T}}\right), \tag{20}$$

where Γ_1 and Γ_2 are real positive definite diagonal matrices and *tr* is the trace function. Deriving Equation (20) gives

$$\dot{V} = \mathrm{e}_\theta^{\mathrm{T}} \dot{e}_\theta + \mathrm{e}_\omega^{\mathrm{T}} J \dot{e}_\omega + tr\left(\tilde{J}_1 \Gamma_1^{-1} \dot{\tilde{J}}_1^{\mathrm{T}} + \tilde{J}_2 \Gamma_2^{-1} \dot{\tilde{J}}_2^{\mathrm{T}}\right),$$

which becomes, when the error derivatives are substituted by Equations (10) and (17)

$$\begin{aligned}\dot{V} = {} & -\mathrm{e}_\theta^{\mathrm{T}} K_\theta e_\theta + \mathrm{e}_\theta^{\mathrm{T}} e_\omega - \mathrm{e}_\omega^{\mathrm{T}} J K_\omega e_\omega + \mathrm{e}_\omega^{\mathrm{T}} J J^{-1} \tilde{J}\left(\dot{\omega}_d - K_\omega e_\omega\right) \\ & - \mathrm{e}_\omega^{\mathrm{T}} J J^{-1} e_\theta \\ & - \mathrm{e}_\omega^{\mathrm{T}} J J^{-1} \operatorname{sgn}\left(\mathrm{e}_\omega\right)\left(\operatorname{sgn}\left(\omega\right)^{\mathrm{T}} \tilde{J}_1 \omega \left\|\omega\right\| + \operatorname{sgn}\left(\omega\right)^{\mathrm{T}} J_1 \omega \left\|\omega\right\| \right. \\ & \left. + \left\|J_2\right\|_{\max} \left\|\omega\right\|^2\right) \\ & - \mathrm{e}_\omega^{\mathrm{T}} J J^{-1} \omega \times J\omega + tr\left(\tilde{J}_1 \Gamma_1^{-1} \dot{\tilde{J}}_1^{\mathrm{T}} + \tilde{J}_2 \Gamma_2^{-1} \dot{\tilde{J}}_2^{\mathrm{T}}\right) \\ = {} & -e_\theta^{\mathrm{T}} K_\theta e_\theta - \mathrm{e}_\omega^{\mathrm{T}} J K_\omega e_\omega - \mathrm{e}_\omega^{\mathrm{T}} \omega \times J\omega \\ & - \mathrm{e}_\omega^{\mathrm{T}} \operatorname{sgn}\left(\mathrm{e}_\omega\right)\left(\operatorname{sgn}\left(\omega\right)^{\mathrm{T}} J_1 \omega \left\|\omega\right\| + \left\|J_2\right\|_{\max} \left\|\omega\right\|^2\right) \\ & + \mathrm{e}_\omega^{\mathrm{T}} \tilde{J}\left(\dot{\omega}_d - K_\omega e_\omega\right) \\ & - \mathrm{e}_\omega^{\mathrm{T}} \operatorname{sgn}\left(\mathrm{e}_\omega\right) \operatorname{sgn}\left(\omega\right)^{\mathrm{T}} \tilde{J}_1 \omega \left\|\omega\right\| + tr\left(\tilde{J}_1 \Gamma_1^{-1} \dot{\tilde{J}}_1^{\mathrm{T}} + \tilde{J}_2 \Gamma_2^{-1} \dot{\tilde{J}}_2^{\mathrm{T}}\right) \\ = {} & -e_\theta^{\mathrm{T}} K_\theta e_\theta - \mathrm{e}_\omega^{\mathrm{T}} J K_\omega e_\omega - \mathrm{e}_\omega^{\mathrm{T}} \omega \times J\omega \\ & - \mathrm{e}_\omega^{\mathrm{T}} \operatorname{sgn}\left(\mathrm{e}_\omega\right)\left(\operatorname{sgn}\left(\omega\right)^{\mathrm{T}} J_1 \omega \left\|\omega\right\| + \left\|J_2\right\|_{\max} \left\|\omega\right\|^2\right) \\ & + tr\begin{pmatrix} \tilde{J}_1\left(\left(\dot{\omega}_d - K_\omega e_\omega\right) \mathrm{e}_\omega^{\mathrm{T}} \right. \\ -\omega \mathrm{e}_\omega^{\mathrm{T}} \operatorname{sgn}\left(\mathrm{e}_\omega\right) \operatorname{sgn}\left(\omega\right)^{\mathrm{T}} \left\|\omega\right\| + \Gamma_1^{-1} \dot{\tilde{J}}_1^{\mathrm{T}}\right) \\ \left. + \tilde{J}_2\left(\left(\dot{\omega}_d - K_\omega e_\omega\right) \mathrm{e}_\omega^{\mathrm{T}} + \Gamma_2^{-1} \dot{\tilde{J}}_2^{\mathrm{T}}\right) \right) .\end{aligned}$$

Applying Equations (18) and (19) of the theorem 3.4 (noting that $\tilde{J} = \hat{J} - J$ leads to $\dot{\tilde{J}} = \dot{\hat{J}}$), it becomes:

$$\begin{aligned}\dot{V} = {} & -e_\theta^{\mathrm{T}} K_\theta e_\theta - \mathrm{e}_\omega^{\mathrm{T}} J K_\omega e_\omega \\ & - \left(\mathrm{e}_\omega^{\mathrm{T}} \operatorname{sgn}\left(\mathrm{e}_\omega\right)\left(\operatorname{sgn}\left(\omega\right)^{\mathrm{T}} J_1 \omega \left\|\omega\right\| + \left\|J_2\right\|_{\max} \left\|\omega\right\|^2\right)\right. \\ & \left. + \mathrm{e}_\omega^{\mathrm{T}} \omega \times J\omega\right).\end{aligned} \tag{21}$$

Equation (12) leads to

$$\left\|\mathrm{e}_\omega\right\| \left\|\omega \times J\omega\right\| \leq \left\|\mathrm{e}_\omega\right\| \left(\operatorname{sgn}\left(\omega\right)^{\mathrm{T}} J_1 \omega \left\|\omega\right\| + \left\|J_2\right\|_{\max} \left\|\omega\right\|^2\right)$$

which gives

$$-\mathrm{e}_\omega^{\mathrm{T}}\omega \times J\omega \leq \mathrm{e}_\omega^{\mathrm{T}}\mathrm{sgn}\,(\mathrm{e}_\omega)\left(\mathrm{sgn}\,(\omega)^{\mathrm{T}} J_1\omega\,\|\omega\| + \|J_2\|_{\max}\,\|\omega\|^2\right)$$
$$\Leftrightarrow 0 \leq \mathrm{e}_\omega^{\mathrm{T}}\mathrm{sgn}\,(\mathrm{e}_\omega)\left(\mathrm{sgn}\,(\omega)^{\mathrm{T}} J_1\omega\,\|\omega\| + \|J_2\|_{\max}\,\|\omega\|^2\right) + \mathrm{e}_\omega^{\mathrm{T}}\omega \times J\omega. \quad (22)$$

Lastly, combining Equations (21) and (22) leads to

$$\dot{V} \leq -e_\theta^{\mathrm{T}} K_\theta e_\theta - \mathrm{e}_\omega^{\mathrm{T}} J K_\omega e_\omega$$

$\dot{V} < 0\,\forall (e_\theta, e_\omega) \in \Re^{*2}$ which proves the asymptotic stability of the system. ■

Lemmata 3.3 and 3.2 are also confirmed.

4. Simulation

In order to assess proposed control, a simulation has been carried out with the parameters of a typical small camera:

$$J = \begin{bmatrix} 0.0015 & 0.0003 & 0.0002 \\ 0.0001 & 0.003 & 0.0003 \\ 0.0002 & 0.0004 & 0.0025 \end{bmatrix}. \quad (23)$$

The control law parameters have been fixed, as follows:

- $K_\theta = 10$
- $K_\omega = 10$
- $\Gamma_1 = 10^{-4}\begin{bmatrix} 1 & 0 & 0 \\ 0 & 1 & 0 \\ 0 & 0 & 1 \end{bmatrix}$
- $\Gamma_2 = 10^{-5}\begin{bmatrix} 1 & 0 & 0 \\ 0 & 1 & 0 \\ 0 & 0 & 1 \end{bmatrix}$.

The adaptive integrations initial values are set to

$$\tilde{J}_1(0) = \begin{bmatrix} 0.001 & 0 & 0 \\ 0 & 0.001 & 0 \\ 0 & 0 & 0.001 \end{bmatrix} \quad (24)$$

and

$$\tilde{J}_2(0) = \begin{bmatrix} 0 & 0 & 0 \\ 0 & 0 & 0 \\ 0 & 0 & 0 \end{bmatrix}.$$

Notice that the sum of those inertia matrices is quite different from the simulated payload inertia matrix exposed in Equation (23). This is done to simulate a payload change in operation without modifying any control parameter.

The simulated ISP system is supposed to be designed for payloads that verify

$$\|J_2\| < \|J_2\|_{\max} = 0.0005.$$

4.1 Path following

The entire control algorithm is proven from the very beginning up to Section 5 since the assessment of the last part would require a real experimentation. A typical expected trajectory is first designed. It consists in drawing a circle around the X-axis with a constant coning angle of $\pi/4$ rad and a rotation speed of $\pi/10\,\mathrm{rad.s}^{-1}$ It is shown with the executed trajectory in Figure 5. One can notice that the control moves the gimbal well to the expected position even if the initial conditions are fully opposite. This observation is reflected in Figure 6. It can be noticed that the trajectory is very smooth, which makes the control particularly suitable for the intended application. It can also be observed that the errors converge very quickly.

The resulting control is exposed in Figure 7. It turns out to be of very small amplitude, which ensures a low energy consumption.

4.2 $\hat{j}$ estimation

Inertial matrix is estimated by integration of Equations (18) and (19). J evolution is shown in Figure 8. It can be seen that all $\hat{J}$ components converge very quickly although they do not necessarily reach their true value. The estimation may be much more precise in real world thanks to vibration noise. However, since reaching these values is not necessary, the result is satisfactory.

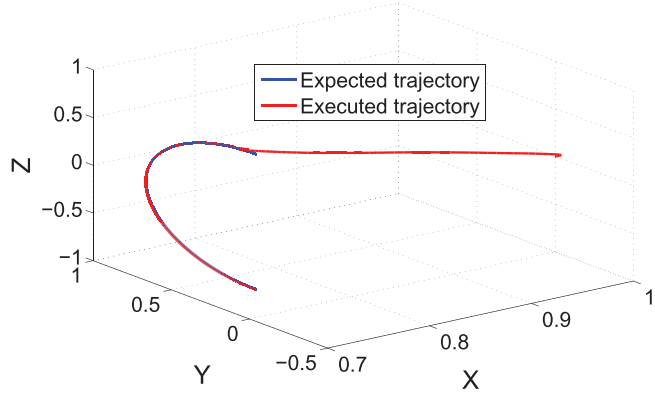

Figure 5. Gimbal trajectory.

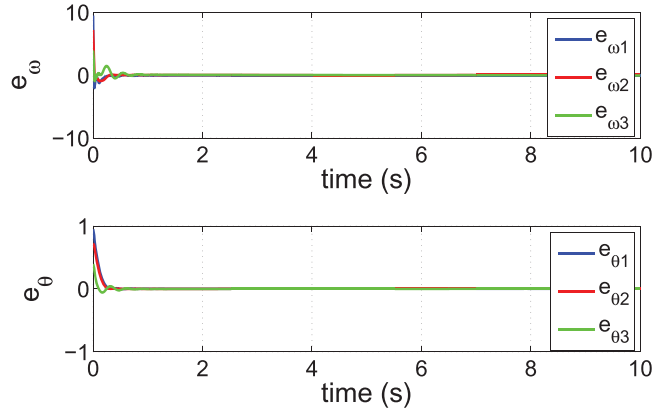

Figure 6. e_θ and e_ω.

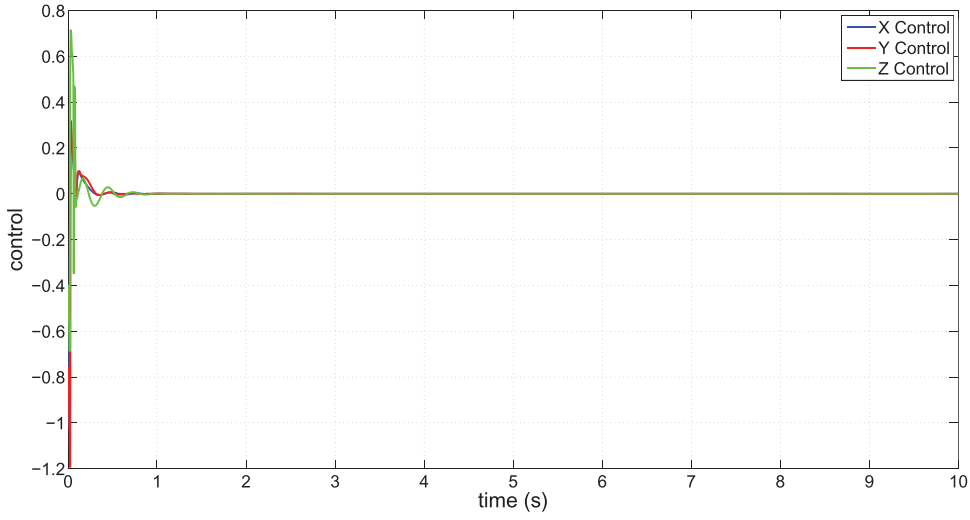

Figure 7. Control response.

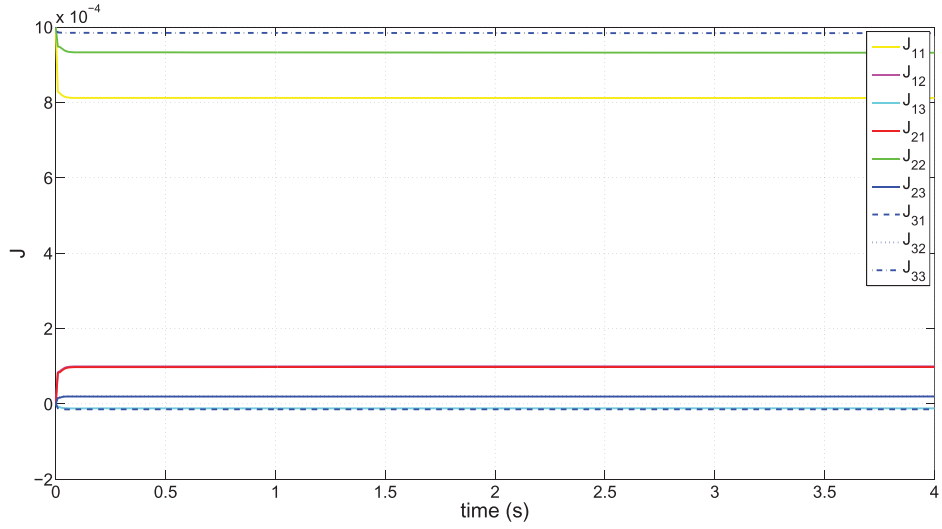

Figure 8. Estimated inertial matrix $\hat{J}$.

4.3 ω error

The error due to ω is balanced following the Sliding Mode idea. Figure 9 shows the obtained control when the expected rotation speed is 10 times greater (i.e. π rad.s^{-1}). It can be seen that, as expected, the control is noisier. However, obtained trajectory remains acceptable as shown in Figure 10. Error amplitude can be greatly reduced by increasing the control gains. This is nevertheless unnecessary as such rotation speed is yet too high to produce a clear film and would only be necessary when switching from one shot to another.

4.4 Adaptive control law interest

The interest of proposed adaptive control law is assessed by comparison with a more conventional law. This latter is obtained deactivating the adaptive law and applying the variables change exposed in Equation (4). Equation (15) is replaced by following control law:

$$\tau = J\left(\dot{\omega}_d - K_\omega e_\omega\right) + \omega \times J\omega - e_\theta,$$

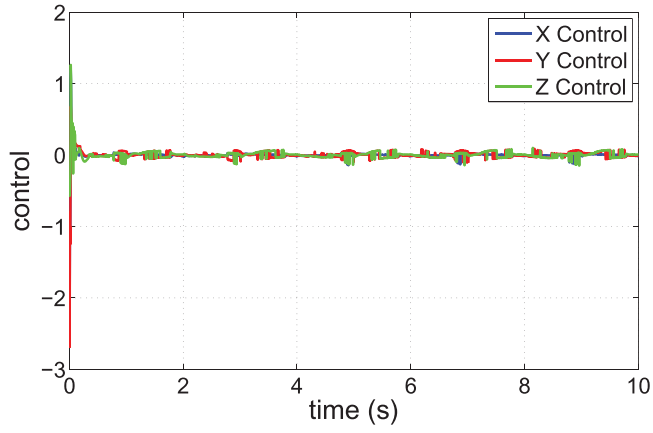

Figure 9. Control response for increased rotation velocity ω.

where J is the expected inertia matrix. The comparison is done in two situations:

- In the same condition as the one exposed at the beginning of Section 4, fixing J to $\tilde{J}_1(0)$ of Equation (24). The error

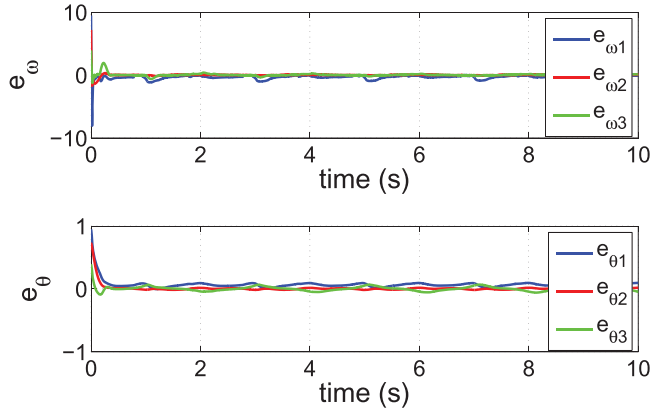

Figure 10. e_θ and e_ω for increased rotation velocity ω.

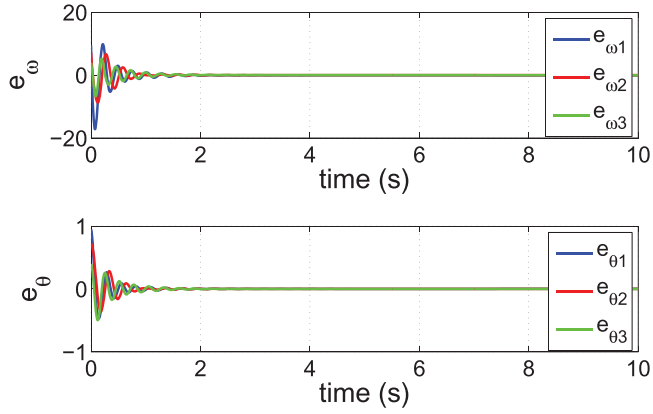

Figure 11. e_θ and e_ω for deactivated adaptation.

evolution is exposed in Figure 11. One can notice that resulting system stabilisation is much slower than the one obtained with adaptive control law.

- Fixing J and $\hat{J}_1(0)$ to

$$J = \hat{J}_1(0) = \begin{bmatrix} 0.0005 & 0 & 0 \\ 0 & 0.0005 & 0 \\ 0 & 0 & 0.0005 \end{bmatrix}.$$

The trajectory obtained from the control with deactivated adaptation is shown in Figure 12. It can be seen that the

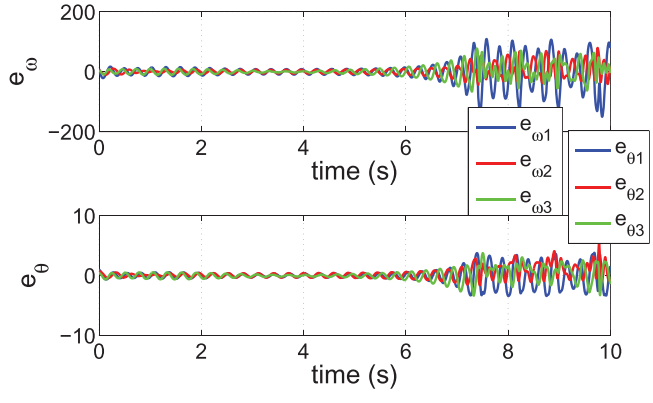

Figure 12. e_θ and e_ω for deactivated adaptation, high inertia matrix error.

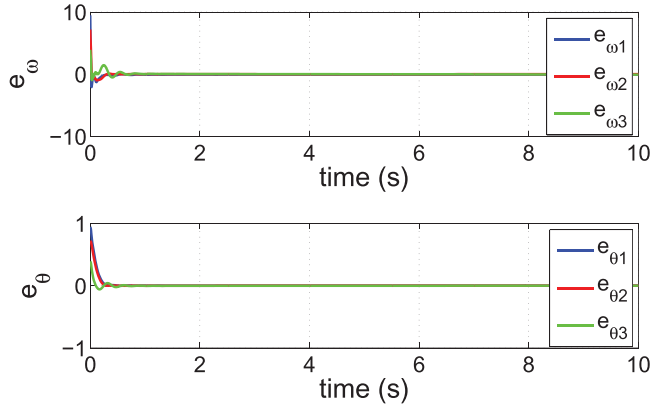

Figure 13. e_θ and e_ω.

control does not manage to stabilise the trajectory to the expected path when the difference between expected and actual inertia matrices is too high. On the other hand, the adaptive control does it very well as demonstrated in Figure 13.

4.5 Relevance in practice

Simulation results detailed in Section 4 seem to prove the suitability of the adaptive approach developed in Section 3 for ISP control. However, ad-hoc tweaks of constants K_θ, K_ω, Γ_1, Γ_2 may be necessary in the future in order to deal with noise, structure deformation, friction, residual unbalance, and other phenomena that have not been taken into account in the considered ideal model (Equation (3)). Parameters used during simulation were indeed chosen arbitrarily.

5. Torque projection

Each engine required torque can be hereafter extracted from the general torque obtained in equation (15). The following few assumptions about gimbal mechanism are made:

- It is well balanced
- It is almost symmetrical
- Its bearing's rotating friction is negligible
- It is of brushless type.

Those assumptions imply that the payload attitude is insensitive to the gimbal base rotating motion. The dynamics chain can, therefore, be only examined starting from the payload up to the base.

Each motor of the intended ISP system is fitted with angular position sensors which enable to correctly orientate the stator magnetic field according to its rotor counterpart. This solution is a bit harder to implement than collocating a second IMU in the base. Nevertheless, it provides the exact motor's rotor position without drift and does not require any additional computing power for filtering.

The first, second and third motors are assumed to be placed, respectively, on payload X -, Y - and Z -axes.[2]

Each frame of the gimbal is numbered starting with 0 for the support of the payload.

5.1 First motor (X-axis)

The first motor required torque τ_{m1} is

$$\tau_{m1} = \begin{bmatrix} 1 \\ 0 \\ 0 \end{bmatrix} \tau.$$

5.2 Second motor (Y -axis)

General torque in frame 1 is first computed. The azimuth of motor 1 is noted θ_{m1}, which is given by the motor angular position sensor (positive when the payload rolls clockwise). Corresponding rotation quaternion q_{m1} is computed as

$$q_{m1} = \mathrm{e}^{\theta_{m1}/2},$$

where $\theta_{m1} = \begin{bmatrix} {}^{l}\theta_{m1} \\ 0 \\ 0 \end{bmatrix}$.

The projection of torque τ on frame 1 is

$$\tau_1' = q_{m1}^* \otimes \tau \otimes q_{m1}.$$

Applying the principle of action/reaction on the effect of motor 1, it leads to

$$\tau_1 = \begin{bmatrix} -1 & 0 & 0 \\ 0 & 1 & 0 \\ 0 & 0 & 1 \end{bmatrix} \tau_1'.$$

Motor 2 must generate required torque τ_1 on top of the torque required to overcome inertia of frame 1. The relation exposed in Equation (3) is applied to frame 1

$$\begin{aligned} \dot{\omega}_1 &= J_1^{-1}\tau_1'' - J_1^{-1}\omega_1 \times J_1\omega_1 \\ \Leftrightarrow \tau_1'' &= J_1\dot{\omega}_1 + \omega_1 \times J_1\omega_1, \end{aligned}$$

where τ_1'' is the torque required to move frame 1. The total torque on frame 1 becomes

$$\tau_1''' = \tau_1 + \tau_1'' = J_1\dot{\omega}_1 + \omega_1 \times J_1\omega_1 + \tau_1.$$

Only ω_1 and $\dot{\omega}$ remains to be computed

$$\omega_1 = \dot{\theta}_{m1} + q_{m1}^* \otimes \omega \otimes q_{m1}.$$

And its derivative is

$$\begin{aligned} \dot{\omega}_1 &= \ddot{\theta}_{m1} + q_{m1}^* \otimes \dot{\omega} \otimes q_{m1} + \frac{1}{2} q_{m1}^* \otimes \omega \otimes q_{m1} \otimes \dot{\theta}_{m1} \\ &\quad - \frac{1}{2}\dot{\theta}_{m1} \otimes q_{m1}^* \otimes \omega \otimes q_{m1} \\ &= \ddot{\theta}_{m1} + q_{m1}^* \otimes \dot{\omega} \otimes q_{m1} + \frac{1}{2}\left(q_{m1}^* \otimes \omega \otimes q_{m1}\right) \otimes \dot{\theta}_{m1} \\ &\quad - \frac{1}{2}\dot{\theta}_{m1}^* \otimes \left(q_{m1}^* \otimes \omega \otimes q_{m1}\right)^* \\ &= \ddot{\theta}_{m1} + q_{m1}^* \otimes \dot{\omega} \otimes q_{m1} + \left(q_{m1}^* \otimes \omega \otimes q_{m1}\right) \times \dot{\theta}_{m1}. \end{aligned}$$

The required torque of motor 2 is thereafter computed as

$$\tau_{m2} = \begin{bmatrix} 0 \\ 1 \\ 0 \end{bmatrix} \tau_1'''.$$

5.3 Third motor (Z-axis)

The third motor required torque assessment is performed following the same method as the second motor as exposed in Section 5.2. Noting θ_{m2} the motor 2 azimuth (positive when the payload pitch upward). The corresponding rotation quaternion q_{m2} is computed as

$$q_{m2} = \mathrm{e}^{\theta_{m2}/2},$$

where $\theta_{m1} = \begin{bmatrix} 0 \\ \theta_{m2} \\ 0 \end{bmatrix}$ The projection of the torque τ on frame 1 is

$$\tau_2' = q_{m2}^* \otimes \tau \otimes q_{m2}.$$

Then applying the principle of action/reaction on the effect of motor 1, it leads to

$$\tau_2 = \begin{bmatrix} 1 & 0 & 0 \\ 0 & -1 & 0 \\ 0 & 0 & 1 \end{bmatrix} \tau_2'.$$

Motor 2 must generate the torque τ_2'''

$$\tau_2''' = J_2\dot{\omega}_2 + \omega_2 \times J_1\omega_2 + \tau_2,$$

where

$$\omega_2 = \dot{\theta}_{m2} + q_{m2}^* \otimes \omega \otimes q_{m2}$$

$$\dot{\omega} = \ddot{\theta}_{m2} + q_{m2}^* \otimes \dot{\omega} \otimes q_{m2} + \left(q_{m2}^* \otimes \omega \otimes q_{m2}\right) \times \dot{\theta}_{m2}.$$

Then the required torque of motor 2 is computed as

$$\tau_{m2} = \begin{bmatrix} 0 \\ 0 \\ 1 \end{bmatrix} \tau_2'''.$$

6. Conclusion

After having exposed the requirements of a new ISP control, an expression in quaternion form of the required orientation that fulfils these requirements is proposed in Section 2. This quaternion form is converted in axis-angle form not to suffer any continuity issue which ensures the absence of any homoclinic-like instability (Chaturvedi et al., 2011). Furthermore, the entire process only requires one trigonometric calculation (i.e. in Equation (7), *ln* function is equivalent to a $\cos^{-1}$ (Morais et al., 2014)) compared to several computations for the classical methods.

A no linear adaptive control law is proposed in Section 3 as well as the necessary conditions to stabilise the system. This control law has the particularity to self-estimate the inertial matrix of its payload, which enables swapping this latter with another payload without any other modification required. The general torque obtained is lastly projected onto each motor axis in Section 5 to complete the control design. A simulation is carried out in the last Section 4 to assess the suitability of proposed control. Outcomes reveal that this latter is very promising both regarding followed path and response speed. It moreover allows installation of a broad range of payload without showing any instability issues.

A prototype is currently under construction to experiment control performances in a real application. It will indeed assess the robustness of the control design with gimbal base displacements.

If the control law has been developed for the gimbal particular application, it is implementable in every kind of systems with dynamics based on quaternion representation (i.e. Equation (3)). For instance, a quadcopter (Carino et al., 2015) would be advantageously controlled by such law to avoid a tedious and time-consuming estimation of its inertia matrix.

References

Cabarbaye, A., Cariño, J., Lozano, R., & Estrada, M. B. (2017). *Fast adaptive control of a 3-DOF inertial stabilized platforms based on quaternions. International Conference on Unmanned Aircraft Systems (ICUAS), Miami, Floride (pp. 219â€“226). Institute of Electrical and Electronics Engineers, IEEE.*

Carino, J., Abaunza, H., & Castillo, P. (2015). *Quadrotor quaternion control*. In International Conference on Unmanned Aircraft Systems (ICUAS), Denver, Colorado (pp. 825–831). Institute of Electrical and Electronics Engineers, IEEE.

Chaturvedi, N. A., Sanyal, A. K., & McClamroch, N. H. (2011). Rigid-body attitude control. *IEEE Control Systems*, *31*(3), 30–51.

Goldstein, H. (1962). *Classical mechanics vol. 4*. Delhi: Pearson Education India.

Hilkert, J. (2008). Inertially stabilized platform technology concepts and principles. *IEEE Control Systems*, *28*(1), 26–46.

Hilkert, J. M., & Hullender, D. A. (1990). April 16–20. *Adaptive control system techniques applied to inertial stabilization systems*. Orlando'90, Orlando, Floride (pp. 190–206). International Society for Optics and Photonics, SPI.

Khalil, H. K. (1996). *Nonlinear systems*. Upper Saddle River: Prentice-Hall.

Khodadadi, H., Motlagh, M. R. J., & Gorji, M. (2011). *Robust control and modeling a 2-dof inertial stabilized platform*. International Conference on Electrical, Control and Computer Engineering (INECCE), Kuantan, Pahang, Malaysia (pp. 223–228). Institute of Electrical and Electronics Engineers, IEEE.

Lee, T. (2013). Robust adaptive attitude tracking on *SO*(3) with an application to a quadrotor UAV. *IEEE Transactions on Control Systems Technology*, *21*(5), 1924–1930.

Lee, T., Leoky, M., & McClamroch, N. H. (2010). *Geometric tracking control of a quadrotor UAV on SE(3)*. 49th IEEE Conference on Decision and Control (CDC), Atlanta, Georgia (pp. 5420–5425). Institute of Electrical and Electronics Engineers, IEEE.

Li, B., & Hullender, D. (1998). Self-tuning controller for nonlinear inertial stabilization systems. *IEEE Transactions on Control Systems Technology*, *6*(3), 428–434.

Mayhew, C. G., Sanfelice, R. G., & Teel, A. R. (2009). *Robust global asymptotic attitude stabilization of a rigid body by quaternion-based hybrid feedback*. Proceedings of the 48th IEEE Conference on Decision and Control, 2009 held jointly with the 28th Chinese Control Conference 2009, CDC/CCC 2009, Shanghai, China (pp. 2522–2527). Institute of Electrical and Electronics Engineers, IEEE.

Morais, J. P., Georgiev, S., & Sprößig, W. (2014). *Real quaternionic calculus handbook*. New Delhi: Springer.

Raptis, I. A., Valavanis, K. P., & Moreno, W. A. (2011). A novel non linear backstepping controller design for helicopters using the rotation matrix. *IEEE Transactions on Control Systems Technology*, *19*(2), 465–473.

Slotine, J.-J. E., Li, W., et al. (1991). Applied nonlinear control (Vol. *199*), Englewood Cliffs, NJ: Prentice-Hall.